Sumoylation of the THO complex regulates the biogenesis of a subset of mRNPs

Hugo Bretes, Jérôme O. Rouvière, Thibaut Leger, Marlene Oeffinger, Frédéric Devaux, Valérie Doye, Benoit Palancade

Published online 5 February 2014 *Nucleic Acids Research, 2014, Vol. 42, No. 8* ***5043–5058***
doi:10.1093/nar/gku124

Sumoylation of the THO complex regulates the biogenesis of a subset of mRNPs

Hugo Bretes[1,2,†], Jérôme O. Rouviere[1,2,†], Thibaut Leger[3], Marlene Oeffinger[4,5,6], Frédéric Devaux[7,8], Valérie Doye[1] and Benoit Palancade[1,*]

[1]Institut Jacques Monod, CNRS, UMR 7592, Univ Paris Diderot, Sorbonne Paris Cité, F-75205 Paris, France, [2]Ecole Doctorale Gènes Génomes Cellules, Université Paris Sud-11, Orsay, France, [3]Proteomics facility, Institut Jacques Monod, CNRS, UMR 7592, Univ Paris Diderot, Sorbonne Paris Cité, F-75205 Paris, France, [4]Department for Systems Biology, Institut de recherches cliniques de Montréal (IRCM), Montreal, Québec, Canada H2W 1R7, [5]Département de Biochimie et Médecine Moléculaire, Faculté de Médecine, Université de Montréal, Montréal, Québec, Canada H3T 1J4, [6]Division of Experimental Medicine, Faculty of Medicine, McGill University, Montréal, Québec, Canada H3A 1A3, [7]Université Pierre et Marie Curie, UMR7238, 15, rue de l'Ecole de Médecine, 75006 Paris, France and [8]CNRS, UMR7238, Laboratoire de Génomique des Microorganismes, 75006 Paris, France

Received October 7, 2013; Revised January 15, 2014; Accepted January 17, 2014

ABSTRACT

Assembly of messenger ribonucleoparticles (mRNPs) is a pivotal step in gene expression, but only a few molecular mechanisms contributing to its regulation have been described. Here, through a comprehensive proteomic survey of mRNP assembly, we demonstrate that the SUMO pathway specifically controls the association of the THO complex with mRNPs. We further show that the THO complex, a key player in the interplay between gene expression, mRNA export and genetic stability, is sumoylated on its Hpr1 subunit and that this modification regulates its association with mRNPs. Altered recruitment of the THO complex onto mRNPs in sumoylation-defective mutants does not affect bulk mRNA export or genetic stability, but impairs the expression of acidic stress-induced genes and, consistently, compromises viability in acidic stress conditions. Importantly, inactivation of the nuclear exosome suppresses the phenotypes of the *hpr1* non-sumoylatable mutant, showing that SUMO-dependent mRNP assembly is critical to allow a specific subset of mRNPs to escape degradation. This article thus provides the first example of a SUMO-dependent mRNP-assembly event allowing a refined tuning of gene expression, in particular under specific stress conditions.

INTRODUCTION

mRNA packaging into messenger ribonucleoparticles (mRNPs) has emerged as a complex and highly regulated process which differentially marks processed molecules, directs them towards export, and dictates their stability, subcellular localization and translation (1). Nuclear mRNP assembly initiates with the cotranscriptional recruitment of mRNA processing factors and several other mRNA-associated proteins, some of which are acting as adaptors for the mRNA-export machinery (2). In budding yeast, Yra1, Nab2 and Npl3 serve as adaptors for the Mex67-Mtr2 export receptor, which ultimately brings mRNPs to the nuclear pore complex (NPC) through interaction with nucleoporins (3). In addition, cotranscriptional mRNP assembly has been shown to involve THO, which is a conserved tetrameric complex comprised of four subunits in yeast—Tho2, Hpr1, Mft1 and Thp2 (4). A pentameric version of THO, including the conserved Tex1 protein, was also recently described (5). The THO complex is associated with active genes and contributes to the recruitment of several mRNA-associated factors, including Sub2, Yra1 (6,7) and SR-like proteins (Gbp2 and Hrb1) (8,9) which together with THO form the so-called TREX (TRanscription and EXport) complex, and Mex67 (10). Most likely as a consequence of improper assembly, mRNPs formed in the absence of the THO complex are retained in the nucleus (7,11,12), and in some cases, degraded by the exosome-associated 3′–5′ exonuclease Rrp6 (13,14). THO complex inactivation also alters transcriptional

*To whom correspondence should be addressed. Tel +33 157 278 061; Fax +33 157 278 063; Email: palancade.benoit@ijm.univ-paris-diderot.fr

†These authors contributed equally to the paper as first authors.

elongation, in particular through G/C-rich, long and/or repeat-containing genes (15–17) and provokes genetic instability, as revealed by hyper-recombination phenotypes (12,18). These phenotypes have been proposed to involve R-loops, which are RNA::DNA hybrids that accumulate in THO mutants (19,20).

As highlighted by several reports, changes in mRNP composition occur precisely at distinct steps of mRNA metabolism (1) whereas improperly assembled mRNPs are carefully evicted in the cells (21,22). However, only a limited number of spatio-temporal regulations targeting mRNP composition have been described. RNA helicase-dependent remodeling is best exemplified by the action of the DEAD-box ATPase Dbp5, which terminates the mRNA export process at the cytoplasmic face of NPCs through displacement of mRNA-associated export factors such as Mex67 and Nab2 (23). In addition, changes in mRNP composition can be driven by mutually exclusive interactions involving mRNA-associated proteins and/or the mRNA itself: Mex67 recruitment by Yra1 disrupts the Yra1-Sub2 interaction *in vitro* (24), while in mammalian cells, mRNA is handed over from adaptors to the export receptor upon formation of a ternary complex (25). Finally, a number of post-translational modifications targeting mRNA-associated proteins were also demonstrated to modulate mRNP content, impacting on mRNP stability and/or nuclear export (26). Among known examples, ubiquitination of Yra1 disrupts its interaction with mRNPs prior to export (27) while Mex67 recruitment onto transcribed genes is facilitated by ubiquitination of the Hpr1 subunit of the THO complex (10).

Protein modification by the small ubiquitin-like modifier SUMO, which has emerged as a key regulator of multiple cellular processes (28), is also susceptible to regulate mRNP assembly. This covalent, reversible modification has already been shown to finely tune several aspects of mRNA metabolism, including transcription and pre-mRNA processing (29,30). In addition, SUMO conjugation often leads to conformational changes or macromolecular complexes rearrangements (31), and could therefore contribute to mRNP remodeling. Finally, a number of enzymes of the SUMO pathway are associated with nuclear pores, which represent the ultimate route for exported mRNPs (30). In particular, mRNPs committed for export are docked at the nuclear basket of NPCs by virtue of their interaction with myosin-like proteins (Mlp) 1 and 2 (32,33), which form a protein platform also contributing to the anchoring of the conserved SUMO-protease Ulp1 (34). Ulp1 (SENP2 in mammals) is an essential SUMO-isopeptidase, which catalyzes both the processing of neosynthesized SUMO prior to conjugation, and the deconjugation of SUMO from its targets (35). A few Ulp1 targets have been identified, but to date, none of them has been associated with mRNA metabolism (35).

Here, we have investigated the involvement of the SUMO pathway, and in particular of the SUMO-protease Ulp1, in mRNP assembly. Through a comprehensive proteomic analysis of mRNP composition, we demonstrate that Ulp1 specifically controls the association of the THO complex with mRNPs. We further show that the THO complex is sumoylated on its Hpr1 subunit in a Ulp1-dependent manner, and that this modification regulates its association with mRNPs. Cells impaired in SUMO-dependent THO complex recruitment exhibit defective expression of acidic stress-inducible genes and, consequently, fail to grow in acidic stress conditions. Importantly, exosome inactivation restores both stress-induced mRNA levels and viability on stress conditions, indicating that defective expression of these mRNAs is caused by mRNA degradation triggered by improper mRNP assembly. This article thus shows that sumoylation of the THO complex regulates mRNP biogenesis, thereby contributing to optimal mRNA expression, as revealed upon specific stress conditions.

MATERIALS AND METHODS

Yeast strains and plasmids

Unless otherwise indicated, all the strains used in this study (listed in Supplementary Table S3) are isogenic to S288C and were grown in liquid culture at 25°C and shifted for 2 h at 30°C. For *GAL* gene induction, 2% galactose was added for 2 h to cells grown in glycerol–lactate (0.17% YNB, 0.5% ammonium sulfate, 0.05% glucose, 2% lactate and 2% glycerol) supplemented with the required nutrients. For weak acid induction, cells were grown on MM4 (minimal medium, pH4) supplemented with 60 mM acetic acid as described (36). When indicated, cycloheximide (100 µg/ml, Sigma) or methylmethane sulfonate (MMS, 0.02%, Sigma) was added to the medium. Construction of plasmids (listed in Supplementary Table S4) was performed using standard molecular cloning techniques. Sequences of oligonucleotides used in this study are available upon request.

mRNP complexes purification

mRNP purification from cells expressing proteinA-tagged baits was performed essentially as described (37). Briefly, frozen grindates were homogenized in nine volumes of extraction buffer (20 mM Hepes pH 7.5, 110 mM KOAc, 2 mM $MgCl_2$, 0.1% Tween-20, 0,5% Triton X-100, 1 mM DTT, 1X protease inhibitors cocktail, complete EDTA-free, Roche and antifoam B, Sigma, 1:5000). When indicated, a 10-min treatment with RNAse A (Sigma, 150 µg/ml) was included. The resulting extract was clarified by filtration through 1.6 µm GD/X Glass Microfiber syringe filters (25mm, Whatman) and further incubated for 30 min at 4°C with IgG-conjugated magnetic beads. Beads were then washed three times with extraction buffer and once with 0.1 M NH_4OAc, 0.1 mM $MgCl_2$, 0.02% Tween-20. Bound-complexes were eluted with 0.5M NH_4OH, 0.5 mM EDTA, lyophilized and resuspended either in SDS-sample buffer for SDS-PAGE or in 25 mM ammonium carbonate for mass spectrometry analysis.

Small-scale immunoprecipitations were performed using IgG-conjugated magnetic beads or anti-HA agarose beads (Pierce). Cells were lysed in the same buffer as above by bead beating using a Fastprep (Qbiogene). After a 10 000-g centrifugation at 4°C for

5 min, the soluble extract was incubated with the beads for 30 min (IgG immunoprecipitation) or 90 min (anti-HA immunoprecipitation) at 4°C. Beads were washed three times with extraction buffer and eluted with SDS sample buffer.

Mass spectrometry analysis

Digestion was performed overnight at 37°C in the presence of 12.5 µg/ml of sequencing grade trypsin (Promega, Madison, Wi, USA). Digests were analyzed by a LTQ Velos Orbitrap (Thermo Fisher Scientific, San Jose, CA) coupled to an Easy nano-LC Proxeon system (Thermo Fisher Scientific, San Jose, CA). Chromatographic separation of peptides was performed with the following parameters: column Easy Column Proxeon C18 (10 cm, 75 µm i.d., 120Å), 300 nl/min flow, gradient rising from 95% solvent A (water—0.1% formic acid) to 25% B (100% acetonitrile, 0.1% formic acid) in 20 min, then to 45% B in 40 min and finally to 80% B in 10 min. Peptides were analyzed in the Orbitrap in full ion scan mode at a resolution of 30 000 and a mass range of 400–1800 m/z. Fragments were obtained with a collision-induced dissociation (CID) activation with a collisional energy of 40%, an activation Q of 0.25 for 10 ms and analyzed in the LTQ. MS/MS data were acquired in a data-dependent mode in which 20 most intense precursor ions were isolated, with a dynamic exclusion of 20 s and an exclusion mass width of 10 ppm. Data were processed with Proteome Discoverer 1.4 software (Thermo Fisher scientific, San Jose, CA) coupled to an in-house Mascot search server (Matrix Science, Boston, MA; version 2.4.1). The mass tolerance of fragment ions was set to 7 ppm for precursor ions and 0.5 Da for fragments. The following modifications were considered in mass calculation: oxidation (M), phosphorylations (STY). The maximum number of missed cleavages was limited to two for trypsin digestion. MS/MS data were searched against the SwissProt database (11/12/13 release) with the *Saccharomyces cerevisiae* taxonomy. Percolator node was used for peptide false discovery rate determination. Peptides were validated when their *q*-value, which represents the minimal false discovery rate at which the identification is considered correct, was below 1%.

Chromatin and RNA immunoprecipitation

Chromatin and RNA immunoprecipitations (ChIP and RIP) were performed using a modified procedure (38). Briefly, cells were cross-linked in the presence of 1% formaldehyde for 10 min at 25°C. After quenching with 100 mM glycine and washing with Tris-buffered saline, the cell pellets were resuspended in 1 ml lysis buffer (50 mM Hepes pH 7.5, 140 mM NaCl, 1 mM EDTA, 1% triton X-100, 0.1% deoxycholate, 1X protease inhibitors cocktail, complete EDTA-free, Roche) and lysis was achieved by bead beating. Cell lysates were collected and split in two parts, respectively, used for ChIP or RIP. When used for ChIP, the cell lysate was further sonicated to shear DNA using a Bioruptor (Diagenode) for two runs of 10 min each and solubilized chromatin was retrieved through a 10 min-centrifugation at 2500 g to prevent differential chromatin fractionation (DCF) (38). When used for RIP, the cell lysate was directly spun at 10 000 g for 5 min at 4°C. Specific antibodies – anti-Hpr1 (39); anti-RNAP II largest subunit (8WG16, Covance)—were added to the relevant soluble extracts and immunoprecipitation was performed by overnight rotation at 4°C. Protein-G sepharose beads (GE Healthcare) were added to the samples for two additional hours. Washes were as follow: twice with lysis buffer, twice with lysis buffer containing 360 mM NaCl; twice with 10 mM Tris pH 8, 250 mM LiCl, 0.5% Nonidet-P40, 0.5% deoxycholate, 1 mM EDTA and once with 10 mM Tris–HCl pH 8, 1 mM EDTA.

Elution was achieved through a 20-min incubation at 65°C in the presence of 50 mM Tris pH 8, 10 mM EDTA, 1% SDS. The eluate was deproteinized with proteinase K (Sigma, 0.2 mg/mL) and uncrosslinked for 30 min at 65°C. Immunoprecipitated nucleic acids (DNA or RNA) were purified with the Qiaquick PCR purification kit (Qiagen) and the Nucleospin RNAII kit (Macherey Nagel), respectively. RNAs were reverse-transcribed with AMV reverse transcriptase (Finnzymes). DNA and cDNA were further quantified by real-time PCR with a LightCycler 480 system (Roche) according to the manufacturer's instructions. Controls without reverse transcriptase allowed estimating the lack of contaminating DNA. RIP (or ChIP) values are the ratios between immunoprecipitated RNA (or DNA) and input RNA (or DNA) amounts. For Hpr1 ChIP, values were further normalized to the ChIP value of RNAP II as described (40). For Hpr1 RIP and ChIP, values were set to 1 for *hpr1Δ* cells (negative control for anti-Hpr1 immunoprecipitation).

DCF analyses were performed as described (41).

SUMO-conjugates isolation

SUMO-conjugates were isolated from yeast cells expressing a His-tagged version of SUMO under the control of the copper-inducible *CUP1* promoter. Briefly, 100 OD600 of cells induced during 4 h in the presence of 0.1 mM CuSO4 were harvested and further processed for nickel agarose denaturing chromatography using reported methods (42) with the following changes. Cells were directly lysed by bead beating in 6 M guanidine HCl, 100 mM sodium phosphate pH8, 10 mM Tris HCl, 0.1% TritonX-100, 10 mM beta-mercaptoethanol, 50 mM N-ethylmaleimide (Sigma). Clarified lysates were incubated with Ni-NTA agarose beads (Qiagen) for 2 h at room temperature. Beads were washed twice with lysis buffer and three times with 8 M urea, 100 mM sodium phosphate, 10 mM Tris HCl pH 6.3 before proceeding to elution.

Western-blot analysis

Total protein extraction from yeast cells was performed by the NaOH–TCA lysis method (42). Samples were separated on 4–12% SDS-PAGE gel and transferred to PVDF membranes. Western-blot analysis was performed using the following antibodies: rabbit IgG-HRP polyclonal antibody (Dakocytomation), 1:5000; monoclonal anti-GFP (Roche Diagnostics), 1:500; monoclonal anti-HA (Covance), 1:1000; monoclonal anti-Pab1

(Santa-Cruz), 1:1000; polyclonal anti-Yra1 (6), 1:1000; polyclonal anti-Nab2 (32), 1:100 000; polyclonal anti-Hpr1 (39), 1:1000; and polyclonal anti-Mex67 (39), 1:50 000. Quantification of signals was performed based on serial dilutions of reference samples using the ImageJ software.

Gene expression analysis

Total RNAs were extracted from yeast cultures using Nucleospin RNA II (Macherey Nagel). For RT-qPCR, RNAs were reverse-transcribed with AMV reverse transcriptase (Finnzymes) and cDNA quantification was achieved through quantitative real-time PCR as above.

For microarray analysis, 1 μg of total RNA was reverse transcribed and labeled with Cy5 or Cy3 using the amino-allyl protocol described at transcriptome.ens.fr/sgdb/protocols/. A set of 52 519 probes matching the ORFs of *S. cerevisiae*, with 1–15 specific probes per gene, was designed using the Teolen software, with default parameters (43). This probe design was deposited on the earray database (AMADID: 027945) and was used to produce Agilent arrays in a 8×60 k format. These Agilent arrays were hybridized with the labeled cDNA using the Agilent hybridization protocol. After washing following the supplier's recommendations, the slides were scanned using a 2-micron Agilent microarray scanner. The images were analyzed using the feature extraction software and normalized by global lowess using Goulphar (44). For each gene, the Cy5/Cy3 ratios corresponding to the different probes were averaged. The *hpr1-KR* versus *wt* comparison was performed twice using independent samples and dye swap. The averaged $\log_2$ of the mutant/wild-type ratios and the standard deviation between the two replicates were calculated for each gene. The genes showing a standard deviation >0.5 were removed from the data. This filter eliminated ~150 genes which were highly variable between replicates. The complete microarray data are available in Supplementary Table S2 and in the ArrayExpress database (www.ebi.ac.uk/arrayexpress) under accession number E-MTAB-2138.

Cells carrying LacZ reporters were lysed and assayed for β-galactosidase activity using the NovaBright™ β-galactosidase Chemiluminescent Detection System (Invitrogen) following the manufacturer's instructions. Relative light units were normalized to the amount of cells as estimated by measurement of the OD at 600 nm.

Miscellaneous

Fluorescence *in situ* hybridization (FISH) was carried out on fixed cells using a Cy3-(dT)50 probe (45). Wide-field fluorescence images were acquired using a DM6000B Leica microscope with a 100×, NA 1.4 (HCX Plan-Apo) oil immersion objective and a CCD camera (CoolSNAP HQ; Photometrics). For Rad52 foci analysis, z-stacks sections of 0.2 μm were acquired using a piezo-electric motor (LVDT; Physik Instrument) mounted underneath the objective lens. Images were scaled equivalently and 3D-projected using MetaMorph 5 (Universal Imaging), and further processed with Photoshop CS2 9.0 software (Adobe).

Hyper-recombination rates were determined as the frequency of deletions of the chromosomal *leu2-k::ADE2-URA3::leu2-k* system based on two 2.16-kb *leu2* repeats as previously described (46).

RESULTS

A proteomic survey of SUMO function in mRNP assembly

To understand the contribution of sumoylation to mRNP assembly and export, we undertook a proteomic analysis of mRNPs isolated from cells carrying a thermosensitive allele of *ULP1* disturbing SUMO-conjugates metabolism (*ulp1-333*, thereafter referred as *ulp1)* (47). The *ulp1* cells exhibit both impaired deconjugation and reduced SUMO processing at semi-restrictive temperature, thereby allowing to assess the global impact of the SUMO pathway on mRNP assembly. Using a reported procedure maintaining mRNP integrity (37), mRNPs were purified from *wt* or *ulp1* cells expressing a tagged version of the small subunit of the nuclear cap-binding complex (Cbp20/Cbc2-protA) and analyzed by SDS-PAGE and silver staining (Figure 1A), or by mass spectrometry (Supplementary Table S1A). Consistent with previous proteomic analysis of Cbp80-associated mRNPs (37), Cbc2-associated proteins purified from *wt* cells included a wide range of mRNAs-associated proteins such as splicing, 3′-end processing and mRNA export factors ($n = 85$, Supplementary Figure S1A and Table S1A). The sensitivity of this proteomic analysis and its selectivity for mRNP components were highlighted by the large number of recovered interactants (Supplementary Table S1A) and the RNAse-sensitive association of most identified proteins (Supplementary Table S1B and Figure S1B), respectively. These analyses revealed that the overall composition of Cbc2-associated mRNPs was not drastically altered upon *ULP1* loss-of-function, indicating that bulk mRNP assembly does not require the SUMO pathway (Figure 1A and B and Supplementary Table S1B). Remarkably however, out of the Cbc2-associated mRNP components whose mass spectrometry scores were strongly altered in the *ulp1* mutant, four corresponded to subunits of the tetrameric THO complex (Tho2, Hpr1, Mft1, Thp2; Supplementary Figure S1A and Table S1B).

To extend our proteomic survey of mRNP composition, we also examined the protein content of nuclear pore-associated mRNPs. Proteomic analysis of Mlp2 interactants unraveled a comprehensive network of proteins including all known nucleoporins, spindle pole body components (48), the 26S proteasome (49) and novel partners (Figure 1D and Supplementary Table S1A). Among them, expanding previous findings (32,33), we identified several mRNP components ($n = 34$), whose RNA-dependent association with nuclear pores was confirmed by RNAse treatment (Supplementary Table S1B and Figure S1C). Importantly, the protein contents of Cbc2- and Mlp2-associated mRNPs were overlapping but clearly distinct (Supplementary Figure S1A and Table S1A),

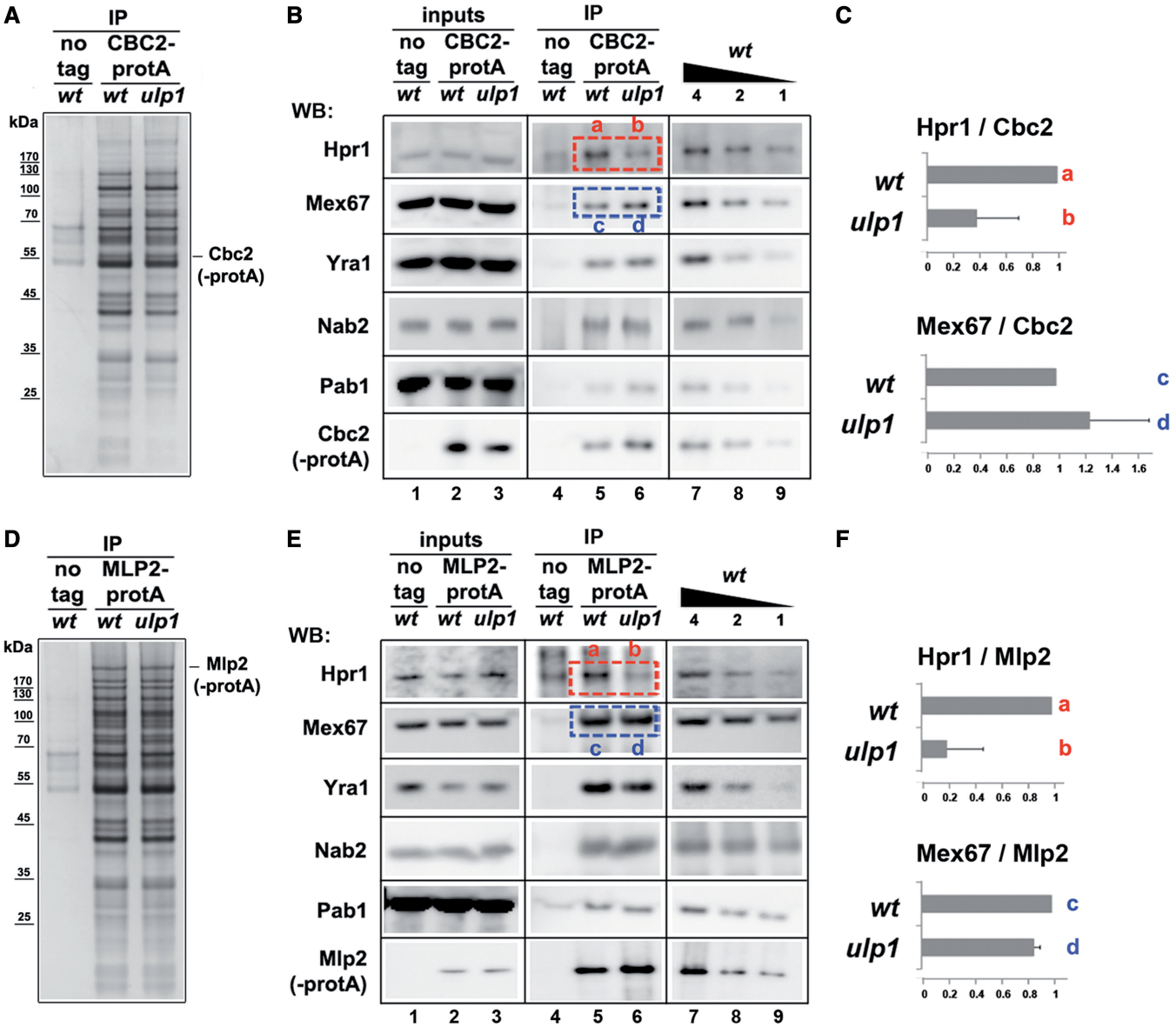

Figure 1. A proteomic survey of SUMO function in mRNP assembly. (**A**) Cbc2-protA associated mRNPs ('IP') isolated from *wt* and *ulp1* cells were analyzed by SDS-PAGE followed by silver staining. Position of the Cbc2-protA-tagged protein is indicated. (**B**) Soluble extracts (left panel, 'inputs') and Cbc2-protA-associated mRNPs (mid panel, 'IP') isolated from *wt* and *ulp*1 cells were analyzed by immunoblotting using the indicated antibodies. Decreasing amounts (µl) of a *wt* reference sample (right panel) were loaded to allow quantification. (**C**) The relative amounts of Hpr1 and Mex67 associated to Cbc2-bound mRNPs (mean ± SD; $n = 2$) were quantified from (B). Signals recorded in 'no tag' lanes were subtracted and values were normalized to the amounts of immunoprecipitated Cbc2 and set to 1 for *wt*. (**D**, **E** and **F**) same as (A, B and C), for Mlp2-protA-associated proteins.

thus validating our approach as appropriate to detect changes in mRNP composition. In particular, Cbc2-associated mRNPs contained multiple splicing factors, whereas, consistent with reported nuclear mRNP remodeling (37), Mlp2-associated mRNPs specifically encompassed late export factors such as Dbp5 or TREX-2 (transcription and export 2, also referred to as THSC), a conserved multi-protein mRNA export factor located to the inner face of NPCs (50). The overall composition of Mlp2-associated mRNPs did not exhibit strong variations upon *ULP1* loss-of-function (Figure 1D and Supplementary Table S1B), indicating that the SUMO pathway is not required for mRNP docking at nuclear pores. However, mass spectrometry scores of the THO complex subunits recovered in the Mlp2-associated mRNPs were also decreased upon *ULP1* loss-of-function (Supplementary Table S1B). This proteomic survey thus identified THO complex subunits as a set of mRNP-associated proteins whose recruitment to both Cbc2- and Mlp2-associated mRNPs could depend on Ulp1 activity, and therefore, on SUMO metabolism. Although Ulp1 may also affect the recruitment of other mRNA-associated factors (Supplementary Table S1B), we focused our subsequent study on the THO complex.

SUMO regulates the association of the THO complex with mRNPs

To validate the predictions from our qualitative proteomic analysis, we used the same Cbc2- and Mlp2-tagged strains for small-scale immunopurifications of mRNPs followed by western-blot analysis with a panel of antibodies for representative mRNP components. This approach confirmed that *ULP1* inactivation decreases the association of the Hpr1 subunit of the THO complex to Cbc2- (Figure 1B and C) and Mlp2-associated mRNPs (Figure 1E and F) while other components (Mex67, Yra1, Nab2, Pab1) remain unaffected. The SUMO pathway is, therefore, specifically required for proper association of the THO complex with mRNPs at various stages of the export process.

In parallel, we examined the recruitment of the THO complex onto specific target mRNAs using RNA immunoprecipitation (RIP) with a specific anti-Hpr1 antibody. Following immunoprecipitation, target mRNAs (*PMA1*, *ADH1*, *YEF3*) selected according to previous genome-wide analysis of THO complex recruitment (17) were quantified by RT-qPCR (Figure 2A). This approach detected a uniform association of the THO complex along mRNAs that decreased upon inactivation of *ULP1* (Figure 2B), further strengthening the outcome of our mRNPs proteomic analysis.

We next used chromatin immunoprecipitation (ChIP) to determine the consequences of *ULP1* inactivation on the recruitment of the THO complex onto RNAP II-transcribed genes (6,7,17). This analysis revealed that the association of the THO complex to its aforementioned target genes (*PMA1*, *ADH1*, *YEF3*) was not altered by *ULP1* loss-of-function (Figure 2C). Our data thus indicate that this SUMO-protease mainly regulates the association of the THO complex with mRNPs.

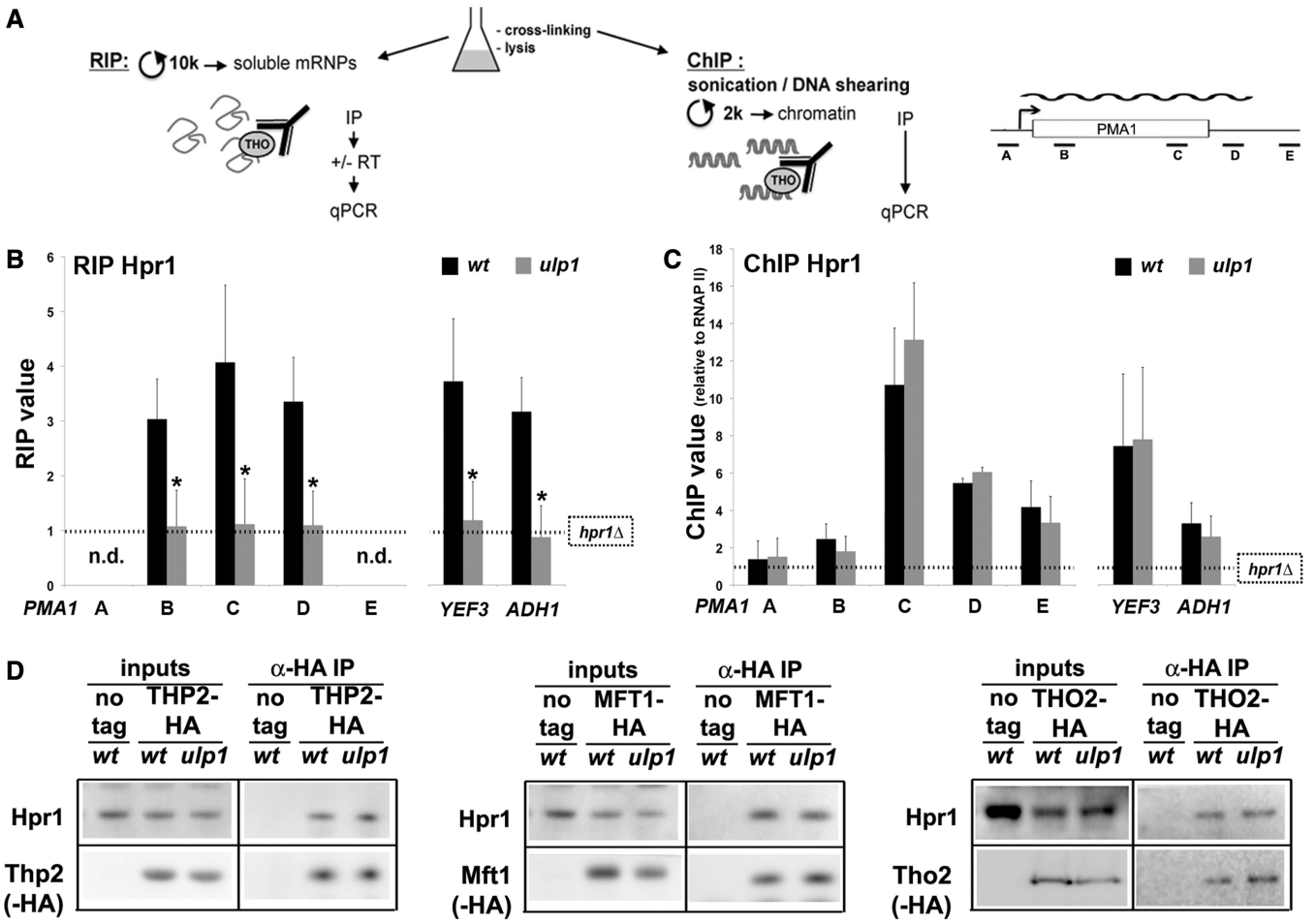

Figure 2. SUMO regulates the recruitment of the whole THO complex within mRNPs. (**A**) RIP and and ChIP experimental design. See Materials and methods section for details. (**B** and **C**) Hpr1 binding onto the indicated mRNAs (B) (RIP Hpr1) and genes (C) (ChIP Hpr1) was quantified by qPCR using specific primer pairs. The positions of the primers along the *PMA1* gene are indicated. RIP (or ChIP) values (mean ± SD; $n = 3$) are the ratios between immunoprecipitated RNA (or DNA) and input RNA (or DNA) amounts. For ChIP, values were further normalized to the ChIP value of RNAP II. In all cases, values were set to 1 for *hpr1Δ* cells (negative control for anti-Hpr1 immunoprecipitation). n.d., not detectable; $*P < 0.05$ (Student's *t*-test). (**D**) Soluble extracts from *wt*, *THP2-HA*, *THP2-HA ulp1*, *MFT1-HA*, *MFT1-HA ulp1*, *THO2-HA or THO2-HA ulp1* cells were used for anti-HA immunoprecipitation. Soluble extracts (left panels, 'inputs') and immunoprecipitated material (right panels, 'α-HA IP') were analyzed by western blotting using anti-Hpr1 (top panels) and anti-HA (lower panels) antibodies. Note that Hpr1 levels are slightly decreased in the presence of HA tags on Mft1 or Tho2; however, each of these HA-tagged subunits coimmunoprecipitate equivalent amounts of Hpr1 from *wt* and *ulp1* extracts.

To determine whether these defects were due to impaired THO complex assembly, immunoprecipitation experiments were carried out in *wt* and *ulp1* cells. This analysis revealed equivalent coimmunoprecipitation of Hpr1 with Thp2, Mft1 or Tho2 subunits, respectively, from *wt* and *ulp1* cell extracts (Figure 2D). These results indicate that the *ulp1* mutant is not affected for bulk THO complex assembly. Taken together, our results therefore establish that the SUMO-protease Ulp1, and consequently the SUMO pathway, contributes to the recruitment of the whole THO complex onto mRNPs.

The THO complex is sumoylated on the C-terminus of its Hpr1 subunit

To determine if the THO complex could be a sumoylated target of Ulp1, cellular SUMO-conjugates were purified by denaturing Ni^{2+} chromatography from strains expressing a poly-histidine-tagged version of SUMO and HA-tagged versions of each of the THO complex subunits. This assay did not detect any sumoylated versions of Tho2, Mft1 and Thp2 subunits (Supplementary Figure S2A). In contrary, small amounts of sumoylated Hpr1 were detectable in SUMO-conjugates fractions from cells coexpressing Hpr1-HA and His-SUMO (Figure 3A, lane 4, compare with lanes 1 and 3). Importantly, sumoylated Hpr1 was also detectable in cells from an unrelated genetic background (W303; Supplementary Figure S2A). These modified forms were unlikely to correspond to ubiquitinated versions of Hpr1, which are solely detectable in the context of proteasome inhibition (39). In addition, these modified forms of Hpr1 were lost upon simultaneous inactivation of the two major SUMO ligases Siz1 and Siz2 (Figure 3B), confirming their sumoylated nature. Importantly, the same approach uncovered an accumulation of sumoylated Hpr1 in *ulp1* mutant cells (Figure 3A, compare lanes 6 and 4), demonstrating that the SUMO-protease Ulp1 targets the THO complex for desumoylation on its Hpr1 subunit.

To further characterize Hpr1 sumoylation, we went on to determine the lysine residues within Hpr1 that are modified by SUMO. For this purpose, we generated several plasmid-based Hpr1 mutants where multiple lysines were mutated to arginines to prevent SUMO conjugation without disturbing the charge of the protein (Figure 3C) and expressed them in *hpr1Δ* cells. Simultaneous mutation of the first 31 (*K1-31R*) or the following 14 (*K32-45R*) lysine residues did not affect the sumoylation level of Hpr1 (Figure 3D, compare lanes 4, 5 and 3). In contrast, mutation of the last 20 lysines within Hpr1 C-terminus (*K46-65R*) completely abolished its sumoylation (Figure 3D, compare lanes 6 and 3). Within this C-terminal domain, mutation of lysine 46–59 (*K46-50R* or *K51-59R*) did not prevent Hpr1 sumoylation, while simultaneous mutation of lysines 60–65 (*K60-65R*) fully abrogated this modification (Figure 3D, compare lanes 10 and 7).

Similar results were obtained when the *hpr1-K60-65R-HA* allele was integrated at the *HPR1* locus (Figure 3E). Within this domain, the SUMOplot software (abgent.com/sumoplot) identified lysine 60 as the unique site with a high probability of modification. However, substitution of lysines 60 and 61 did not affect Hpr1 sumoylation in our *in vivo* assay (H. Bretes *et al.*, unpublished results). This is in agreement with numerous reports where mutation of single lysines does not abrogate monosumoylation and results in sumoylation at an adjacent site (51–53). Taken together, our results thus indicate that the THO complex is sumoylated on the C-terminus of Hpr1.

THO complex sumoylation occurs independent of its ubiquitination

Ubiquitination was previously demonstrated to target Hpr1 for proteasomal degradation (39). In conditions where sumoylated Hpr1 readily accumulates (e.g. in the *ulp1* mutant, Figure 3A), the degradation rates of Hpr1 or other THO complex subunits were not altered (Figure 4A and B). Similarly, in conditions where Hpr1 sumoylation is prevented (e.g. in the *siz1 siz2* SUMO ligase mutant, or in the *hpr1-K60-65R* mutant, see Figure 3B and E), the global turnover of Hpr1 remained unaffected (Figure 4C and D). These results thus demonstrate that sumoylation of Hpr1 neither prevents, nor stimulates its ubiquitin-dependent degradation.

In contrast, simultaneous mutations of lysines 51–59 led to a strong accumulation of the Hpr1 protein (Figure 4E and F; see also Figure 3D, compare lane 9 and 7, or 19 and 17), indicating that these lysines likely contribute to Hpr1 ubiquitin-dependent proteasomal degradation. Importantly, the Hpr1-K51-59R mutant protein was still sumoylated (Figure 3D), showing that Hpr1 ubiquitination does not modulate its sumoylation. Of note, Hpr1 C-terminus (residues 548–752) was identified as a partner of the ubiquitin-associated domain of Mex67 in the two-hybrid assay (10) and Hpr1 degradation was shown to be slowed down upon deletion of its last 88 aminoacids (39). Together with our results, these data strongly suggest that within lysine 51–59, lysines 58 and 59 are the major residues involved in ubiquitin-dependent degradation of Hpr1 (Figure 4G).

Interestingly, secondary-structure-prediction programs detect with a high probability the presence of an intrinsically disordered domain in this region of the Hpr1 protein (residues 667–752; Supplementary Figure S2B). Such domains have been demonstrated to be particularly prone to modification by ubiquitin (54) and ubiquitin-like modifiers (55). Together, our data reveal that ubiquitination and sumoylation occur independently on distinct residues within a short and likely disordered domain at the C-terminus of Hpr1.

THO complex sumoylation regulates its association with mRNPs

Although *HPR1* deletion differentially impacted viability depending on the temperature and the genetic background, these growth defects were fully rescued by expression of the Hpr1-K60-65R protein (Figure 5A). Since this allele does not impair Hpr1 ubiquitination and complements *HPR1* deletion, it was further used as a specific

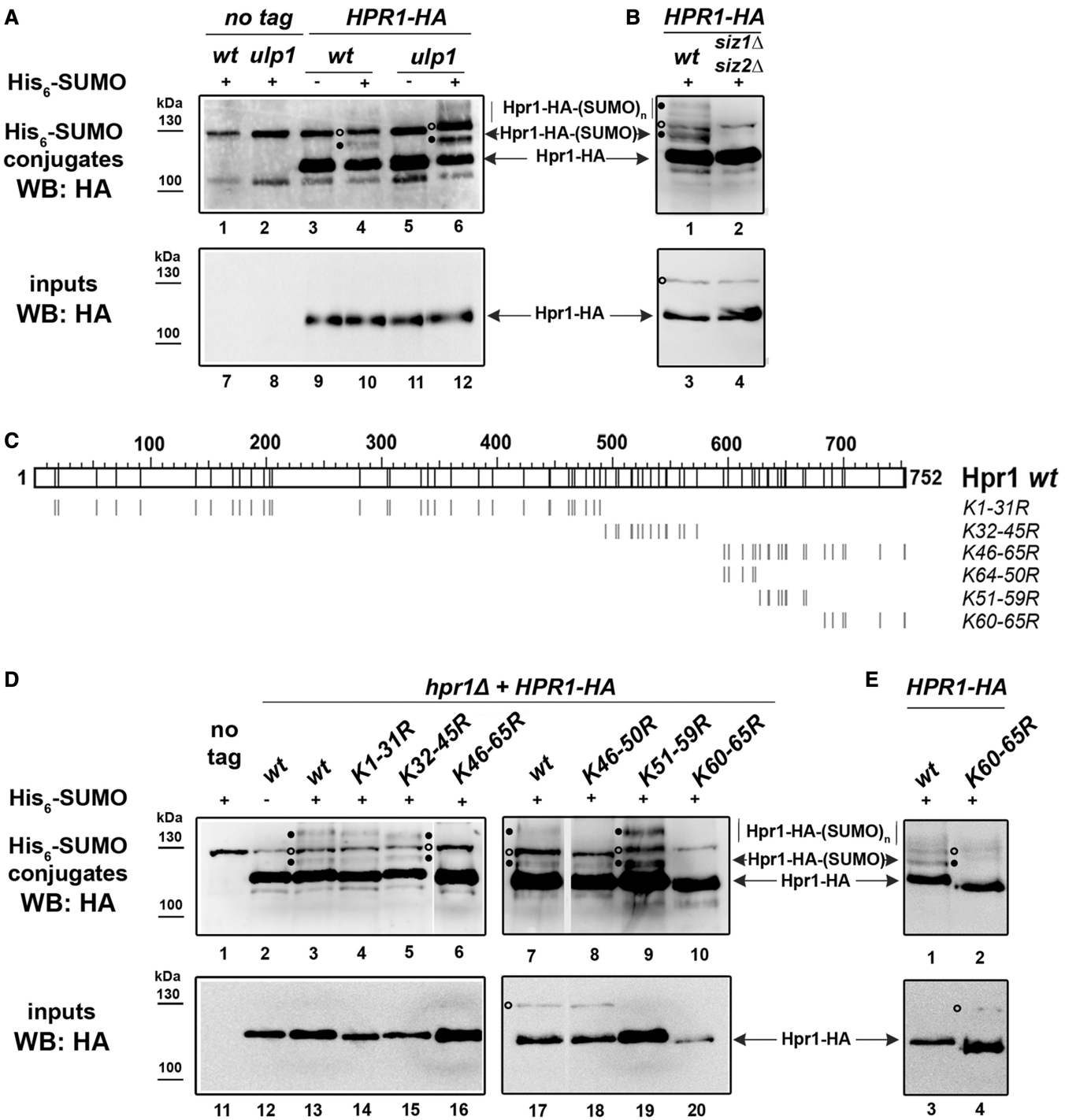

Figure 3. The THO complex is sumoylated on the C-terminus of its Hpr1 subunit. (**A**) Denatured lysates from *wt* or *ulp1* cells expressing a HA-tagged version of Hpr1 and/or a His-tagged version of SUMO (+/−) were used for nickel chromatography. Total lysates ('inputs', bottom panel) and purified His-SUMO conjugates (top panel) were analyzed by western blotting using anti-HA antibodies. Closed circles show the position of sumoylated Hpr1. Open circles show the position of an anti-HA non-specific reactive band. Note that the non-specific binding of a fraction of non-sumoylated Hpr1-HA (also observed in the absence of His-SUMO, lanes 3 and 5) is a classical issue in SUMO-conjugates purification (see Supplementary Figure S2A). (**B**) The same analysis as in (A) was performed with lysates from *wt* and *siz1Δ siz2Δ* cells expressing His-SUMO (+). (**C**) Design of the *hpr1-KR* mutant alleles. The positions of the lysine residues mutated in these mutants are indicated by dashes along the protein sequence. (**D**) The same analysis as in (A) was performed with lysates from *hpr1Δ* cells expressing plasmid-borne lysine mutants of HA-tagged Hpr1 and/or His-SUMO (+/−). Total lysates ('inputs', bottom panels) and purified His-SUMO conjugates (top panels) were analyzed by western blotting using anti-HA antibodies. (**E**) The same analysis as in (D) was performed with lysates from cells expressing a genomically HA-tagged version of Hpr1, either *wt* or *K60-65R*. Molecular weights are indicated (kDa).

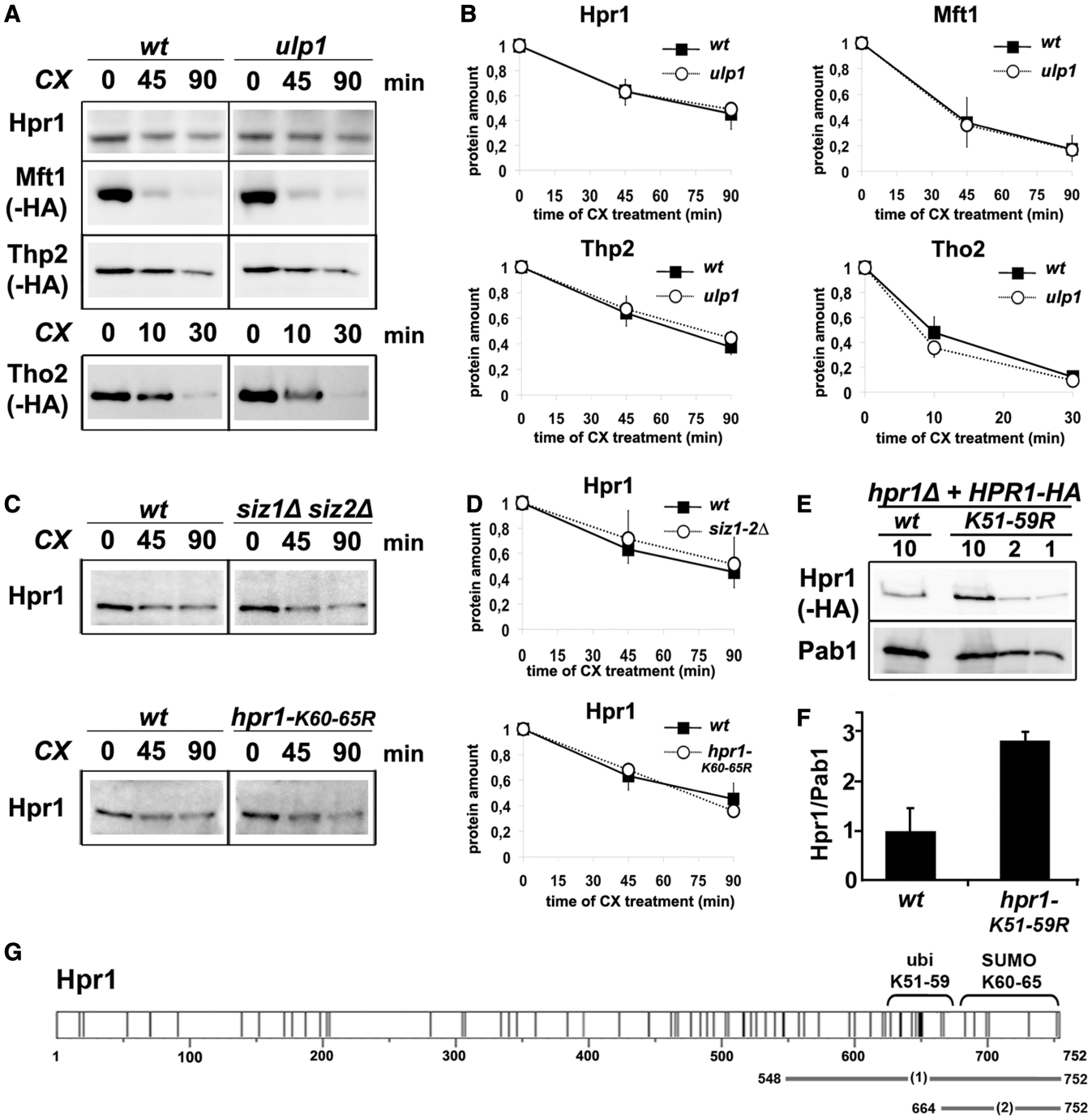

Figure 4. THO complex sumoylation occurs independent of its ubiquitin-dependent degradation. (**A**) Protein levels of Hpr1- and HA-tagged versions of other THO complex subunits were analyzed in *wt* and *ulp1* cells treated with cycloheximide (CX) for the indicated time (minutes). Whole cell extracts were analyzed by western blotting using anti-Hpr1 or anti-HA antibodies. (**B**) The relative amounts of the indicated proteins (mean ± SD; $n = 3$) were quantified over time in *wt* and *ulp1* cells following CX treatment. The quantities of proteins were determined using ImageJ and are expressed relative to $t = 0$. Note that the different THO subunits exhibit distinct half-lives; however, their decay is overall similar in *wt* and *ulp1* cells. (**C**) Same as (A), in *wt*, *siz1Δ siz2Δ* and *hpr1-K60-65R* cells. (**D**) Same as (B), in *wt*, *siz1Δ siz2Δ* and *hpr1-K60-65R* cells. (**E**) Protein levels of Hpr1 were analyzed in *hpr1Δ* cells expressing HA-tagged versions of wt Hpr1 or Hpr1-K51-59R. Whole-cell extracts (decreasing amounts, in µl) were analyzed by western blotting using anti-HA (top panel) and anti-Pab1 (lower panel) antibodies. (**F**) The amounts of Hpr1 (relative to the loading control Pab1, mean ± SD; $n = 2$) were determined using ImageJ. (**G**) Map of Hpr1 lysine residues. The domains encompassing the lysine residues targeted by sumoylation ('SUMO, K60-65') or required for ubiquitin-dependent turnover ('ubi, K51-59') are indicated. [1] Interaction domain reported for Mex67 ubiquitin-associated domain (UBA) (10); [2] domain deleted in the reportedly stabilized *hpr1Δ88* mutant (39). Numbers refers to the amino acid positions.

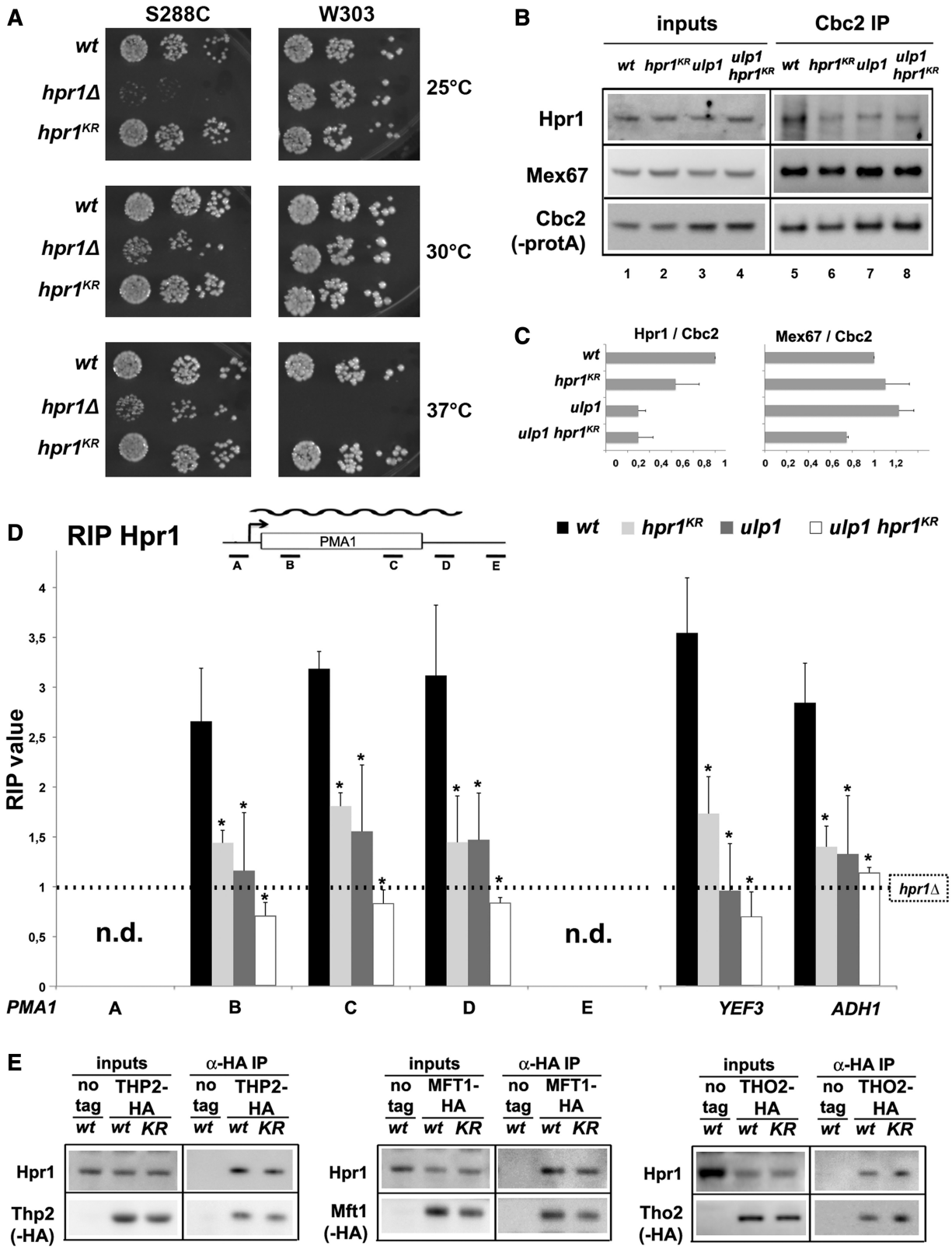

Figure 5. THO complex sumoylation regulates its association with mRNPs. (**A**) Serial dilutions of the indicated strains were grown on YPD plates at the indicated temperature (*hpr1*^{KR} = *hpr1-K60-65R*). The genetic background is indicated (S288C or W303). (**B**) Soluble extracts (left panel, 'inputs') and Cbc2-protA associated mRNPs (right panel, 'IP') isolated from the indicated strains were analyzed by immunoblotting using the indicated antibodies. (**C**) The relative amounts of Hpr1 and Mex67 associated to Cbc2-bound mRNPs were quantified from (B). Values (mean ± SD; $n = 2$) were normalized to the amounts of immunoprecipitated Cbc2 and set to 1 for *wt*. (**D**) Hpr1 binding onto the indicated mRNAs was quantified in the indicated strains by RIP using an anti-Hpr1 antibody followed by RT-qPCR using specific primer pairs. The positions of the primers along the *PMA1* gene are indicated. RIP values (mean ± SD; $n = 3$) are the ratios between immunoprecipitated and input RNA amounts. Values were set to 1

(continued)

non-sumoylatable *hpr1* mutant in our next studies (subsequently referred to as *hpr1-KR*).

To evaluate the impact of Hpr1 sumoylation on THO complex association with mRNAs, we analyzed the recruitment of the *hpr1-KR* mutant protein into Cbc2-associated mRNPs. This revealed a reduced association of the non-sumoylatable *hpr1-KR* protein with mRNPs as compared to *wt* Hpr1 (Figure 5B, compare lanes 5 and 6; Figure 5C). To better quantify this decreased recruitment, we performed RIP in the same mutants (Figure 5D). This approach confirmed the reduced association of the non-sumoylatable *hpr1-KR* mutant with its target mRNAs (Figure 5D). Both approaches further revealed that unlike in *HPR1* wt cells, the decreased recruitment observed in *hpr1-KR* cells was not further enhanced by *ULP1* inactivation (Figure 5B, compare lanes 6 and 8; Figure 5C and D). This strongly supports that a sumoylation/desumoylation cycle occurring on the C-terminal domain of Hpr1 contributes to its recruitment onto mRNPs.

Importantly, sumoylation did not impair the bulk association of Hpr1 with the THO complex, as revealed by the similar coimmunoprecipitation of both Hpr1 and hpr1-KR with HA-tagged Thp2, Mft1 or Tho2 (Figure 5E). Although we cannot formally exclude that the assembly of the specific mRNP-associated fraction of the THO complex could be altered in *hpr1-KR* and *ulp1* mutants, our data indicate that Hpr1 sumoylation likely regulates the recruitment of the entire THO complex onto mRNPs.

THO complex sumoylation does not impact on genetic stability and bulk mRNA export

In view of the described functions of the THO complex, we next analyzed the consequences of impaired Hpr1 sumoylation on genetic stability, mRNA export and mRNA expression. Unlike THO-inactivation mutants (*hpr1Δ*) (18), mutants affecting THO complex sumoylation (*hpr1-KR*, *ulp1*) do not display increased recombination between direct chromosomal repeats (Supplementary Figure S3A). In addition, impairing sumoylation of Hpr1 does not lead to synthetic lethality when combined with DNA damage checkpoint mutants (Supplementary Figure S3B and H. Bretes *et al.*, unpublished results), a phenotype previously reported for THO null mutants (56). Finally, unlike *hpr1Δ* cells (56), *hpr1-KR* cells do not exhibit an increased occurrence of DNA double-strand break-repair foci labeled by Rad52 (Supplementary Figure S3C). Taken together, these data show that THO complex sumoylation does not impact on genetic stability.

Recruitment of known THO complex-dependent mRNP components such as Mex67 was not detectably affected by changes in Hpr1 sumoylation in the *ulp1* or *hpr1-KR* mutants (see Figures 1B and E and 5B). In agreement with these biochemical data, the *ulp1* and *hpr1-KR* mutants did not exhibit bulk mRNA export defects, as probed by FISH analysis of poly-A+ RNAs (Supplementary Figure S4A). These results indicate that while THO complex sumoylation regulates its own association with mRNPs, it does not further affect mRNP export.

THO complex sumoylation is required for the expression of stress-inducible genes and for viability upon stress conditions

To gain insight into the impact of THO complex sumoylation on gene expression, we first analyzed the expression of the bacterial LacZ gene, a reporter typically affected in THO mutants. Beta-galactosidase assays revealed a mild yet significant reduction of LacZ expression in *hpr1-KR* cells as compared to *wt* (Supplementary Figure S4B).

This result prompted us to characterize the impact of THO complex sumoylation on endogenous gene expression. Total RNAs were extracted from *wt* and *hpr1-KR* cells and transcriptome profiles were analyzed by microarray. Preventing Hpr1 sumoylation (*hpr1-KR*) did not cause extensive changes in gene expression at the genomic level (Figure 6A). Indeed, only 41 genes exhibited mRNA levels at least 1.5-fold above or below the *wt* values in *hpr1-KR* cells (Supplementary Table S2), thus differing from the reported genome-wide impact of THO inactivation (811 genes affected in *hpr1Δ* cells) (17). In addition, only a very limited number of genes exhibited consistent changes between two replicate experiments. Among them, the only clear functional enrichment was observed for genes involved in the adaptive response to chemical stresses caused by lowered pH (Haa1 regulon). These genes (*YRO2*, *TPO2*, *TDA6*, *HSP30*, *YLR297w*, *YDR222w*, *TPO3*, indicated on Figure 6A) were therefore selected for further studies.

To confirm that Hpr1 sumoylation is required for the expression of this subset of genes, *wt* and *hpr1-KR* cells were grown in conditions of induction of the Haa1 regulon, e.g. minimal media (MM4) supplemented with acetic acid (36). In agreement with previous reports (57), acid treatment lead to an increased expression of the considered genes in *wt* cells, as revealed by RT-qPCR (*YRO2*, *TDA6*, *TPO2*, *TPO3* panels; Figure 6B). Importantly, *hpr1-KR* cells specifically exhibited reduced mRNA levels for these genes (Figure 6B, compare with the *ACT1* panel).

Expression of genes of the Haa1 regulon is essential for cell survival upon acidic stress (36). Strikingly, impairing Hpr1 sumoylation (*hpr1-KR*) similarly affected viability

Figure 5. Continued
for *hpr1Δ* cells (negative control for anti-Hpr1 immunoprecipitation). n.d., not detectable. $*P < 0.05$ (Student's *t*-test, compared to *wt*). (**E**) Soluble extracts from *wt*, *THP2-HA*, *THP2-HA hpr1-KR*, *MFT1-HA*, *MFT1-HA hpr1-KR*, *THO2-HA or THO2-HA hpr1-KR* cells were used for anti-HA immunoprecipitation. Soluble extracts (left panels, 'inputs') and immunoprecipitated material (right panels, 'α-HA IP') were analyzed by western blotting using anti-Hpr1 (top panels) and anti-HA (lower panels) antibodies. Note that Hpr1 levels are slightly decreased in the presence of HA tags on Mft1 or Tho2; however, each of these HA-tagged subunits coimmunoprecipitate equivalent amounts of Hpr1 from *wt* and *hpr1-KR* extracts.

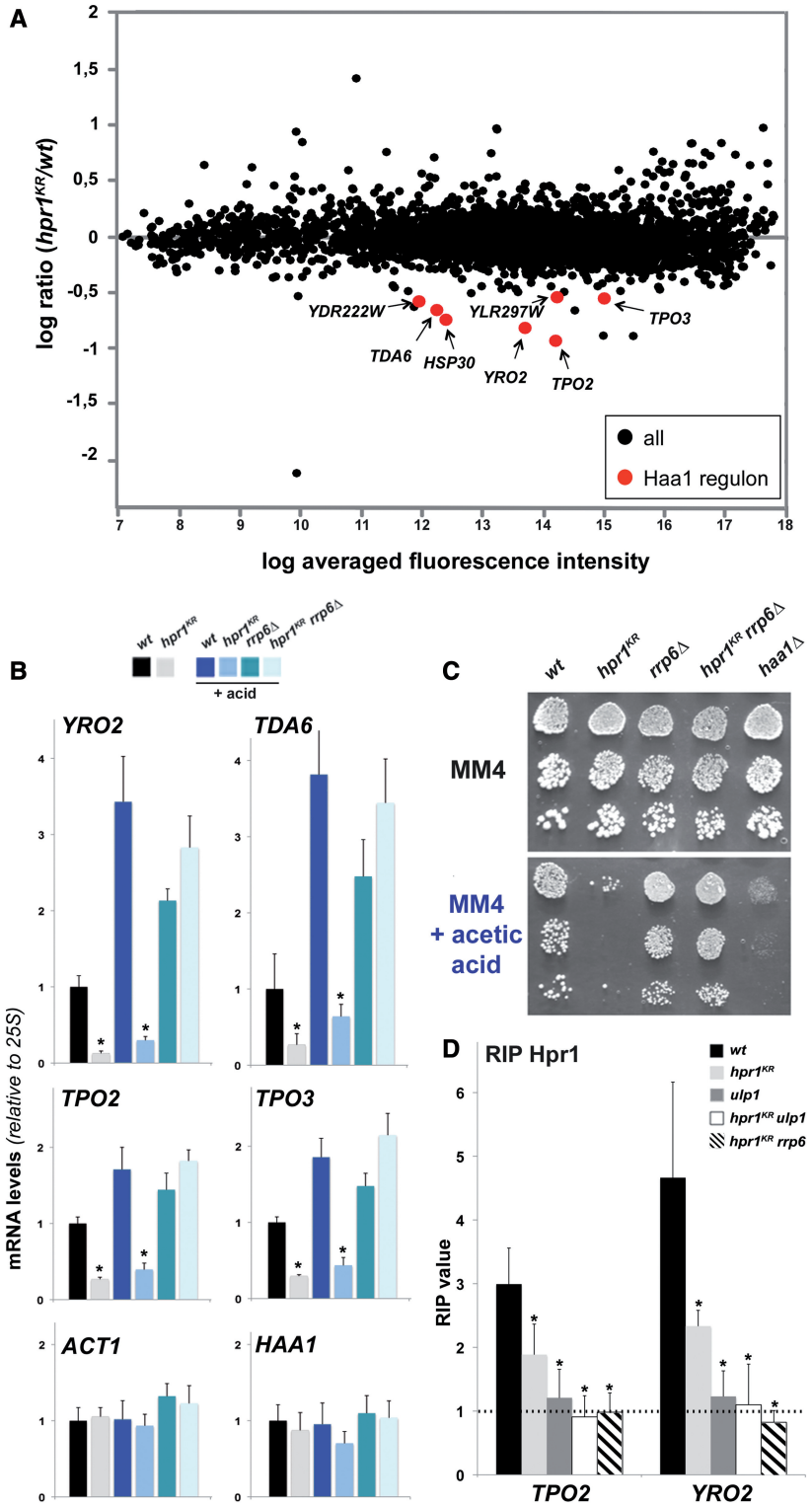

Figure 6. THO complex sumoylation is required for the expression of stress-inducible genes and for viability upon stress conditions. (**A**) Transcriptome analysis of the *hpr1-KR* mutant (MA plot). The *Y*-axis (M) is the averaged $\log_2$ of the *hpr1-KR*/wt ratios calculated from two independent microarray hybridizations. The *X*-axis (A) is the $\log_2$ of the averaged fluorescence intensities. The genes belonging to the Haa1 regulon, which have been further investigated, are highlighted. The complete dataset used to draw this graph is available in Supplementary Table S2. (**B**) mRNA levels for the *YRO2*, *TDA6*, *TPO2*, *TPO3*, *ACT1* and *HAA1* genes were measured by RT-qPCR (normalized to 25S rRNA values, mean ± SD; $n = 3$) in the indicated strains grown in MM4 medium and treated or not for 30 min with 60 mM acetic acid. $^*P < 0.05$ (Student's *t*-test, compared to *wt*). (**C**) Serial dilutions of the indicated strains were grown at 30°C on MM4 solid medium supplemented or not with 60 mM acetic acid. (**D**) Hpr1 binding onto the indicated mRNAs was quantified by RIP using an anti-Hpr1 antibody followed by RT-qPCR using specific primer pairs. RIP values (mean ± SD; $n = 3$) are the ratios between immunoprecipitated and input RNA amounts. Values were set to 1 (dotted line) for *hpr1Δ* cells (negative control for anti-Hpr1 immunoprecipitation). $^*P < 0.05$ (Student's *t*-test, compared to *wt*).

on acetic acid-containing media (Figure 6C). Notably, the growth defect of *hpr1-KR* cells recorded on acid-containing media was also observed in an unrelated genetic background, albeit to a lower extent (W303; Supplementary Figure S5A). However, this phenotype did not reflect a general sensitivity of the *hpr1-KR* mutant to stress conditions (Supplementary Figure S5B). In particular, unlike THO inactivation mutants (13), *hpr1-KR* cells did not display heat sensitivity (Figure 5A) or 3′-end degradation of the heat-shock induced *HSP104* transcript (Supplementary Figure S5C). Taken together, our results thus establish that Hpr1 sumoylation is critical for the optimal expression of a subset of stress-inducible genes (e.g. the Haa1 regulon) and subsequently, for viability in the corresponding stress conditions.

Improperly assembled mRNPs are targeted for degradation by the exosome in THO sumoylation mutants

We first confirmed that sumoylation of Hpr1 also regulates THO complex association with acid-induced mRNAs. RIP analyses indeed revealed that both *hpr1-KR* and *ulp1* cells exhibit decreased association of the THO complex with *TPO2* and *YRO2* mRNAs (Figure 6D).

The expression of this subset of genes is notably regulated by the Haa1 transcriptional activator (58). However, *hpr1-KR* cells were not affected for the expression of the *HAA1* mRNA (Figure 6B). In addition, the effect of the *hpr1-KR* mutant was observed both in uninduced and acid-induced conditions (Figure 6B). Furthermore, RNAP II recruitment along acid-induced genes was not affected in *hpr1-KR* cells (Supplementary Figure S5D). These results therefore suggest that the observed effects on the Haa1 regulon in *hpr1-KR* cells are post-transcriptional.

To assess whether improper mRNP assembly triggers increased degradation of mRNAs of the Haa1 regulon, the *hpr1-KR* allele was combined with the inactivation of the Rrp6 subunit of the exosome. *RRP6* deletion clearly suppressed the mRNA expression defect in *hpr1-KR* cells, restoring the amounts of *YRO2*, *TDA6*, *TPO2* and *TPO3* acid-induced mRNAs to levels comparable with *wt* (Figure 6B). Importantly, while *RRP6* inactivation rescued *TPO2* and *YRO2* mRNAs levels in *hpr1-KR* cells, it did not restore Hpr1 association to these mRNAs (Figure 6D), further strengthening the fact that exosomal degradation occurs as a consequence of decreased Hpr1 recruitment. Moreover, *RRP6* deletion suppressed the strong viability defect of *hpr1-KR* cells on acid-containing media (Figure 6C). Taken together, our data thus establish that in THO sumoylation mutants, improperly assembled mRNPs of the Haa1 regulon are targeted for degradation by the exosome.

In THO-inactivation mutants, exosome-mediated degradation of *HSP* transcripts was previously reported to be associated with defective mRNP release from the transcription site. This leads to the persistence of the corresponding genomic loci at the vicinity of the NPC, giving rise to a detectable chromatin heterogeneity referred to as DCF (38). While we detected DCF formation both at *HSP104* and acid-induced genes loci upon THO inactivation, this phenotype was not recorded in *hpr1-KR* cells (Supplementary Figure S5E). Loss of THO complex sumoylation therefore triggers defects in mRNP assembly and stability for acid-induced mRNAs without detectable mRNP retention (as probed by DCF).

DISCUSSION

While an increasing number of post-translational modifications have been reported to influence mRNP assembly (26), we describe for the first time the involvement of SUMO in this process. Indeed, we show that the Hpr1 subunit of the THO complex is sumoylated on its C-terminus, and that its sumoylation/desumoylation regulates the association of the THO complex with mRNPs. Distinct mechanisms may account for the intriguing finding that both the non-sumoylatable *(hpr1-KR)* and the hyper-sumoylated *(ulp1)* mutants display decreased THO recruitment on mRNPs (Figure 5).

On one hand, SUMO was already reported to modify the interaction properties of its target proteins with nucleic acids, either DNA (59) or RNA (52,60). Hpr1 sumoylation could directly interfere with the nucleic-acid binding properties of the THO complex, for example by preventing the recently demonstrated interaction between Tho2 C-terminus and DNA/RNA (5). Interestingly, Siz1 and Siz2, the SUMO ligases for Hpr1 (Figure 3B), have been reported to bind DNA through their SAP domain (61,62). For genes at the nuclear periphery, an Hpr1 sumoylation–desumoylation cycle driven by chromatin-bound SUMO ligases and NPC-bound Ulp1 could be necessary for mRNA recognition by the THO complex.

On the other hand, sumoylation–desumoylation could be part of complex formation, as suggested by the fact that several transcription factors are recruited into co-repressor complexes in a SUMO-dependent manner, but do not appear to be sumoylated in the final assembly (63). Likewise, Hpr1 sumoylation could modulate the interaction of the THO complex with an unknown protein partner involved in its recruitment onto mRNPs. Interestingly, sumoylation of intrinsically disordered domains such as the one encompassing Hpr1 SUMO acceptor sites has been proposed to create novel interaction surfaces (51) which, in the case of the THO complex, would allow mRNP binding. Following this initial recruitment, desumoylation of Hpr1 could remodel the mRNP, resulting in stable association of the THO complex. Of note, these different scenarios would involve a transient sumoylation of the THO complex, which is consistent with the detection of low levels of sumoylated Hpr1 in wt cells (Figure 3A).

Our data further revealed that sumoylation of Hpr1 is largely independent from its ubiquitination-dependent turnover (Figure 4). However, other post-translational modifications could also control THO complex activity as reported for other mRNA-associated factors (26). For instance, DNA damage-induced phosphorylation of the THO complex was reported to trigger its dissociation from RNA in mammalian cells (64). Spatio-temporal

coordination of these post-translational modifications is also expected to be critical for mRNP fate. Strikingly, the only conserved enzymes reported to associate with nuclear pores are the SUMO-protease Ulp1 and the RNA helicase Dbp5, which both target mRNPs-associated factors. Mechanisms ensuring a local activation of Dbp5 at the cytoplasmic face of nuclear pores have been extensively documented (23). While it is tempting to speculate that Ulp1-dependent remodeling could occur at the nuclear basket, a free fraction of Ulp1 may also perform this task in the nucleoplasm. In both hypotheses, physiological conditions of disturbed Ulp1 localization (65,66) could influence mRNP composition.

In agreement with an overall normal mRNP composition, *ulp1* and *hpr1-KR* mutants do not display any mRNA export defects (Supplementary Figure S4), suggesting that the loading of mRNA export factors onto mRNPs is fully supported by the chromatin-associated THO complex fraction, or compensated by redundant pathways (67,68). In contrast, we have demonstrated that SUMO-dependent control of THO complex recruitment onto mRNAs is critical for acidic stress-induced gene expression. Indeed, *hpr1-KR* cells exhibit strongly reduced levels of mRNAs of the acid-induced, Haa1-dependent regulon and do not survive on acid-containing media. Altered expression of this subset of genes thus likely accounts for the previously reported identification of the *hpr1Δ* and *thp2Δ* THO inactivation mutants in several genome-wide screens for weak acid sensitive strains (69–71). The fact that expression of the *HAA1* regulator itself and RNAP II recruitment along acid-induced genes were not affected in *hpr1-KR* cells suggested that the observed effects on the Haa1 regulon could be post-transcriptional. Consistently, inactivation of the exosome (*rrp6Δ*) was shown to restore acid-induced mRNAs levels in the *hpr1-KR* mutant. These results indicate that in *wt* cells, SUMO-dependent recruitment of the THO complex allows this specific subset of mRNPs to escape exosomal degradation, either by directly protecting the mRNA, or by contributing to the recruitment of other mRNP-associated factors that would not have been uncovered in our proteomic analysis of bulk mRNP composition. Interestingly, sub-optimal mRNP assembly has already been proposed to trigger exosome-mediated degradation of heat shock-induced *HSP* mRNAs in THO deletion mutants (13,72). Of note, THO null mutants are extremely sick in combination with exosome inactivation (13), suggesting that the failure to degrade improperly assembled mRNPs is detrimental. In contrast, *hpr1-KR* cells, which have more limited defects in mRNP assembly, are not sensitive to exosome inactivation under normal growth conditions. Moreover, *RRP6* deletion rescues the lethality of *hpr1-KR* cells on acid-containing media, likely by restoring normal levels of mRNAs of the Haa1 regulon.

mRNAs which are affected upon impairment of THO function share the common feature of being strongly expressed, in particular in response to stress (13,17,38,41). Indeed, strong bursts of mRNP production might be highly sensitive to any alterations in mRNP packaging arising upon THO dysfunction. However, loss of Hpr1 sumoylation does not affect the levels of any abundant or stress-induced mRNAs. Additional features of acid-induced genes of the Haa1 regulon may render their mRNAs more sensitive to degradation in *hpr1-KR* cells. This might include particular chromatin environment, nuclear positioning or secondary RNA structures that could also favor exosomal degradation upon improper mRNP packaging. While the initial identification of this specific subset of genes in our transcriptome analysis is due to the fact that they are already down-regulated in uninduced *hpr1-KR* cells, other mRNAs, not expressed in our conditions, may also require Hpr1 sumoylation for proper expression. In the future, detailed analysis of mRNP composition for specific mRNAs will be required to further refine the role of THO complex sumoylation in mRNP assembly, both in normal and environmentally challenged cells.

SUPPLEMENTARY DATA

Supplementary Data are available at NAR online.

ACKNOWLEDGEMENT

We are very grateful to the Institut Jacques Monod Proteomics Platform, to A. Johnston for technical help and to A. Aguilera, A. Corbett, C. Dargemont, D. Libri, V. Geli, M.C. Geoffroy, M. Hochstrasser, A. Jacquier, L. Pintard, R. Rothstein, M. Rout and F. Stutz for sharing reagents and/or discussion. Thanks to L. Jourdren for the probe design of the *Saccharomyces cerevisiae* arrays used in this study and to G. Lelandais for help with data normalization.

FUNDING

Centre National de la Recherche Scientifique (to B.P. and V.D.); the Fondation ARC pour la Recherche sur le Cancer ('Projet ARC' 2012 and 2013 to B.P.); the Ligue Nationale contre le Cancer (Comité d'Ile de France, to B.P.); CIHR (to M.O.); PhD fellowships from Ministère de l'Enseignement Supérieur et de la Recherche (to H.B. and J.O.R.) and the Fondation ARC pour la Recherche sur le Cancer (to H.B.). Funding for open access charges: Fondation ARC pour la Recherche sur le Cancer.

Conflict of interest statement. None declared.

REFERENCES

1. Muller-McNicoll,M. and Neugebauer,K.M. (2013) How cells get the message: dynamic assembly and function of mRNA-protein complexes. *Nat. Rev. Genet.*, **14**, 275–287.
2. Luna,R., Rondon,A.G. and Aguilera,A. (2012) New clues to understand the role of THO and other functionally related factors in mRNP biogenesis. *Biochim. Biophys. Acta.*, **1819**, 514–520.
3. Oeffinger,M. and Zenklusen,D. (2012) To the pore and through the pore: A story of mRNA export kinetics. *Biochim. Biophys. Acta.*, **1819**, 494–506.
4. Chavez,S., Beilharz,T., Rondon,A.G., Erdjument-Bromage,H., Tempst,P., Svejstrup,J.Q., Lithgow,T. and Aguilera,A. (2000)

A protein complex containing Tho2, Hpr1, Mft1 and a novel protein, Thp2, connects transcription elongation with mitotic recombination in Saccharomyces cerevisiae. *EMBO J.*, **19**, 5824–5834.
5. Pena,A., Gewartowski,K., Mroczek,S., Cuellar,J., Szykowska,A., Prokop,A., Czarnocki-Cieciura,M., Piwowarski,J., Tous,C., Aguilera,A. *et al.* (2012) Architecture and nucleic acids recognition mechanism of the THO complex, an mRNP assembly factor. *EMBO J.*, **31**, 1605–1616.
6. Zenklusen,D., Vinciguerra,P., Wyss,J.C. and Stutz,F. (2002) Stable mRNP formation and export require cotranscriptional recruitment of the mRNA export factors Yra1p and Sub2p by Hpr1p. *Mol. Cell Biol.*, **22**, 8241–8253.
7. Strasser,K., Masuda,S., Mason,P., Pfannstiel,J., Oppizzi,M., Rodriguez-Navarro,S., Rondon,A.G., Aguilera,A., Struhl,K., Reed,R. *et al.* (2002) TREX is a conserved complex coupling transcription with messenger RNA export. *Nature*, **417**, 304–308.
8. Hurt,E., Luo,M.J., Rother,S., Reed,R. and Strasser,K. (2004) Cotranscriptional recruitment of the serine-arginine-rich (SR)-like proteins Gbp2 and Hrb1 to nascent mRNA via the TREX complex. *Proc. Natl Acad. Sci. USA*, **101**, 1858–1862.
9. Hacker,S. and Krebber,H. (2004) Differential export requirements for shuttling serine/arginine-type mRNA-binding proteins. *J. Biol. Chem.*, **279**, 5049–5052.
10. Gwizdek,C., Iglesias,N., Rodriguez,M.S., Ossareh-Nazari,B., Hobeika,M., Divita,G., Stutz,F. and Dargemont,C. (2006) Ubiquitin-associated domain of Mex67 synchronizes recruitment of the mRNA export machinery with transcription. *Proc. Natl Acad. Sci. USA*, **103**, 16376–16381.
11. Guo,S., Hakimi,M.A., Baillat,D., Chen,X., Farber,M.J., Klein-Szanto,A.J., Cooch,N.S., Godwin,A.K. and Shiekhattar,R. (2005) Linking transcriptional elongation and messenger RNA export to metastatic breast cancers. *Cancer Res.*, **65**, 3011–3016.
12. Dominguez-Sanchez,M.S., Barroso,S., Gomez-Gonzalez,B., Luna,R. and Aguilera,A. (2011) Genome instability and transcription elongation impairment in human cells depleted of THO/TREX. *PLoS Genet.*, **7**, e1002386.
13. Libri,D., Dower,K., Boulay,J., Thomsen,R., Rosbash,M. and Jensen,T.H. (2002) Interactions between mRNA export commitment, 3′-end quality control, and nuclear degradation. *Mol. Cell Biol.*, **22**, 8254–8266.
14. Rougemaille,M., Gudipati,R.K., Olesen,J.R., Thomsen,R., Seraphin,B., Libri,D. and Jensen,T.H. (2007) Dissecting mechanisms of nuclear mRNA surveillance in THO/sub2 complex mutants. *EMBO J.*, **26**, 2317–2326.
15. Li,Y., Wang,X., Zhang,X. and Goodrich,D.W. (2005) Human hHpr1/p84/Thoc1 regulates transcriptional elongation and physically links RNA polymerase II and RNA processing factors. *Mol. Cell Biol.*, **25**, 4023–4033.
16. Voynov,V., Verstrepen,K.J., Jansen,A., Runner,V.M., Buratowski,S. and Fink,G.R. (2006) Genes with internal repeats require the THO complex for transcription. *Proc. Natl Acad. Sci. USA*, **103**, 14423–14428.
17. Gomez-Gonzalez,B., Garcia-Rubio,M., Bermejo,R., Gaillard,H., Shirahige,K., Marin,A., Foiani,M. and Aguilera,A. (2011) Genome-wide function of THO/TREX in active genes prevents R-loop-dependent replication obstacles. *EMBO J.*, **30**, 3106–3119.
18. Jimeno,S., Rondon,A.G., Luna,R. and Aguilera,A. (2002) The yeast THO complex and mRNA export factors link RNA metabolism with transcription and genome instability. *EMBO J.*, **21**, 3526–3535.
19. Huertas,P. and Aguilera,A. (2003) Cotranscriptionally formed DNA:RNA hybrids mediate transcription elongation impairment and transcription-associated recombination. *Mol. Cell*, **12**, 711–721.
20. Stirling,P.C., Chan,Y.A., Minaker,S.W., Aristizabal,M.J., Barrett,I., Sipahimalani,P., Kobor,M.S. and Hieter,P. (2012) R-loop-mediated genome instability in mRNA cleavage and polyadenylation mutants. *Genes Dev.*, **26**, 163–175.
21. Fasken,M.B. and Corbett,A.H. (2009) Mechanisms of nuclear mRNA quality control. *RNA Biol.*, **6**, 237–241.
22. Schmid,M. and Jensen,T.H. (2013) Transcription-associated quality control of mRNP. *Biochim. Biophys. Acta.*, **1829**, 158–168.
23. Folkmann,A.W., Noble,K.N., Cole,C.N. and Wente,S.R. (2011) Dbp5, Gle1-IP6, and Nup159: a working model for mRNP export. *Nucleus*, **2**, 540–548.
24. Strasser,K. and Hurt,E. (2001) Splicing factor Sub2p is required for nuclear mRNA export through its interaction with Yra1p. *Nature*, **413**, 648–652.
25. Hautbergue,G.M., Hung,M.L., Golovanov,A.P., Lian,L.Y. and Wilson,S.A. (2008) Mutually exclusive interactions drive handover of mRNA from export adaptors to TAP. *Proc. Natl Acad. Sci. USA*, **105**, 5154–5159.
26. Tutucci,E. and Stutz,F. (2011) Keeping mRNPs in check during assembly and nuclear export. *Nat. Rev. Mol. Cell Biol.*, **12**, 377–384.
27. Iglesias,N., Tutucci,E., Gwizdek,C., Vinciguerra,P., Von Dach,E., Corbett,A.H., Dargemont,C. and Stutz,F. (2010) Ubiquitin-mediated mRNP dynamics and surveillance prior to budding yeast mRNA export. *Genes Dev.*, **24**, 1927–1938.
28. Geiss-Friedlander,R. and Melchior,F. (2007) Concepts in sumoylation: a decade on. *Nat. Rev. Mol. Cell Biol.*, **8**, 947–956.
29. Vethantham,V. and Manley,J.L. (2009) Emerging roles for SUMO in mRNA processing and metabolism. In *SUMO Regulation of Cellular Processes*. Springer, Dordrecht, pp. 41–57.
30. Rouviere,J.O., Geoffroy,M.C. and Palancade,B. (2013) Multiple crosstalks between mRNA biogenesis and SUMO. *Chromosoma*, **122**, 387–399.
31. Gareau,J.R. and Lima,C.D. (2010) The SUMO pathway: emerging mechanisms that shape specificity, conjugation and recognition. *Nat. Rev. Mol. Cell Biol.*, **11**, 861–871.
32. Green,D.M., Johnson,C.P., Hagan,H. and Corbett,A.H. (2003) The C-terminal domain of myosin-like protein 1 (Mlp1p) is a docking site for heterogeneous nuclear ribonucleoproteins that are required for mRNA export. *Proc. Natl Acad. Sci. USA*, **100**, 1010–1015.
33. Vinciguerra,P., Iglesias,N., Camblong,J., Zenklusen,D. and Stutz,F. (2005) Perinuclear Mlp proteins downregulate gene expression in response to a defect in mRNA export. *EMBO J.*, **24**, 813–823.
34. Zhao,X., Wu,C.Y. and Blobel,G. (2004) Mlp-dependent anchorage and stabilization of a desumoylating enzyme is required to prevent clonal lethality. *J. Cell Biol.*, **167**, 605–611.
35. Palancade,B. and Doye,V. (2008) Sumoylating and desumoylating enzymes at nuclear pores: underpinning their unexpected duties? *Trends Cell Biol.*, **18**, 174–183.
36. Fernandes,A.R., Mira,N.P., Vargas,R.C., Canelhas,I. and Sa-Correia,I. (2005) Saccharomyces cerevisiae adaptation to weak acids involves the transcription factor Haa1p and Haa1p-regulated genes. *Biochem. Biophys. Res. Commun.*, **337**, 95–103.
37. Oeffinger,M., Wei,K.E., Rogers,R., DeGrasse,J.A., Chait,B.T., Aitchison,J.D. and Rout,M.P. (2007) Comprehensive analysis of diverse ribonucleoprotein complexes. *Nat. Methods*, **4**, 951–956.
38. Rougemaille,M., Dieppois,G., Kisseleva-Romanova,E., Gudipati,R.K., Lemoine,S., Blugeon,C., Boulay,J., Jensen,T.H., Stutz,F., Devaux,F. *et al.* (2008) THO/Sub2p functions to coordinate 3′-end processing with gene-nuclear pore association. *Cell*, **135**, 308–321.
39. Gwizdek,C., Hobeika,M., Kus,B., Ossareh-Nazari,B., Dargemont,C. and Rodriguez,M.S. (2005) The mRNA nuclear export factor Hpr1 is regulated by Rsp5-mediated ubiquitylation. *J. Biol. Chem.*, **280**, 13401–13405.
40. Abruzzi,K.C., Lacadie,S. and Rosbash,M. (2004) Biochemical analysis of TREX complex recruitment to intronless and intron-containing yeast genes. *EMBO J.*, **23**, 2620–2631.
41. Mouaikel,J., Causse,S.Z., Rougemaille,M., Daubenton-Carafa,Y., Blugeon,C., Lemoine,S., Devaux,F., Darzacq,X. and Libri,D. (2013) High-frequency promoter firing links THO complex function to heavy chromatin formation. *Cell Rep.*, **5**, 1082–1094.
42. Ulrich,H.D. and Davies,A.A. (2009) In vivo detection and characterization of sumoylation targets in Saccharomyces cerevisiae. *Methods Mol. Biol.*, **497**, 81–103.
43. Jourdren,L., Duclos,A., Brion,C., Portnoy,T., Mathis,H., Margeot,A. and Le Crom,S. (2010) Teolenn: an efficient and customizable workflow to design high-quality probes for microarray experiments. *Nucleic Acids Res.*, **38**, e117.

44. Lemoine,S., Combes,F., Servant,N. and Le Crom,S. (2006) Goulphar: rapid access and expertise for standard two-color microarray normalization methods. *BMC Bioinform.*, **7**, 467.
45. Chadrin,A., Hess,B., San Roman,M., Gatti,X., Lombard,B., Loew,D., Barral,Y., Palancade,B. and Doye,V. (2010) Pom33, a novel transmembrane nucleoporin required for proper nuclear pore complex distribution. *J. Cell Biol.*, **189**, 795–811.
46. Piruat,J.I. and Aguilera,A. (1996) Mutations in the yeast SRB2 general transcription factor suppress hpr1-induced recombination and show defects in DNA repair. *Genetics*, **143**, 1533–1542.
47. Lewis,A., Felberbaum,R. and Hochstrasser,M. (2007) A nuclear envelope protein linking nuclear pore basket assembly, SUMO protease regulation, and mRNA surveillance. *J. Cell Biol.*, **178**, 813–827.
48. Niepel,M., Strambio-de-Castillia,C., Fasolo,J., Chait,B.T. and Rout,M.P. (2005) The nuclear pore complex-associated protein, Mlp2p, binds to the yeast spindle pole body and promotes its efficient assembly. *J. Cell Biol.*, **170**, 225–235.
49. Niepel,M., Molloy,K.R., Williams,R., Farr,J.C., Meinema,A.C., Vecchietti,N., Cristea,I.M., Chait,B.T., Rout,M.P. and Strambio-De-Castillia,C. (2013) The nuclear basket proteins Mlp1p and Mlp2p are part of a dynamic interactome including Esc1p and the proteasome. *Mol. Biol. Cell*, **24**, 3920–3938.
50. Garcia-Oliver,E., Garcia-Molinero,V. and Rodriguez-Navarro,S. (2012) mRNA export and gene expression: the SAGA-TREX-2 connection. *Biochim. Biophys. Acta.*, **1819**, 555–565.
51. Bielska,K., Seliga,J., Wieczorek,E., Kedracka-Krok,S., Niedenthal,R. and Ozyhar,A. (2012) Alternative sumoylation sites in the Drosophila nuclear receptor Usp. *J. Steroid. Biochem. Mol. Biol.*, **132**, 227–238.
52. Maison,C., Bailly,D., Roche,D., Montes de Oca,R., Probst,A.V., Vassias,I., Dingli,F., Lombard,B., Loew,D., Quivy,J.P. *et al.* (2011) SUMOylation promotes de novo targeting of HP1alpha to pericentric heterochromatin. *Nat. Genet.*, **43**, 220–227.
53. Figueroa-Romero,C., Iniguez-Lluhi,J.A., Stadler,J., Chang,C.R., Arnoult,D., Keller,P.J., Hong,Y., Blackstone,C. and Feldman,E.L. (2009) SUMOylation of the mitochondrial fission protein Drp1 occurs at multiple nonconsensus sites within the B domain and is linked to its activity cycle. *FASEB J.*, **23**, 3917–3927.
54. Radivojac,P., Vacic,V., Haynes,C., Cocklin,R.R., Mohan,A., Heyen,J.W., Goebl,M.G. and Iakoucheva,L.M. (2010) Identification, analysis, and prediction of protein ubiquitination sites. *Proteins*, **78**, 365–380.
55. Xie,H., Vucetic,S., Iakoucheva,L.M., Oldfield,C.J., Dunker,A.K., Obradovic,Z. and Uversky,V.N. (2007) Functional anthology of intrinsic disorder. 3. Ligands, post-translational modifications, and diseases associated with intrinsically disordered proteins. *J. Proteome Res.*, **6**, 1917–1932.
56. Gomez-Gonzalez,B., Felipe-Abrio,I. and Aguilera,A. (2009) The S-phase checkpoint is required to respond to R-loops accumulated in THO mutants. *Mol. Cell Biol.*, **29**, 5203–5213.
57. Mira,N.P., Becker,J.D. and Sa-Correia,I. (2010) Genomic expression program involving the Haa1p-regulon in Saccharomyces cerevisiae response to acetic acid. *OMICS*, **14**, 587–601.
58. Mira,N.P., Teixeira,M.C. and Sa-Correia,I. (2010) Adaptive response and tolerance to weak acids in Saccharomyces cerevisiae: a genome-wide view. *OMICS*, **14**, 525–540.
59. Hardeland,U., Steinacher,R., Jiricny,J. and Schar,P. (2002) Modification of the human thymine-DNA glycosylase by ubiquitin-like proteins facilitates enzymatic turnover. *EMBO J.*, **21**, 1456–1464.
60. Vassileva,M.T. and Matunis,M.J. (2004) SUMO modification of heterogeneous nuclear ribonucleoproteins. *Mol. Cell Biol.*, **24**, 3623–3632.
61. Parker,J.L., Bucceri,A., Davies,A.A., Heidrich,K., Windecker,H. and Ulrich,H.D. (2008) SUMO modification of PCNA is controlled by DNA. *EMBO J.*, **27**, 2422–2431.
62. Psakhye,I. and Jentsch,S. (2012) Protein group modification and synergy in the SUMO pathway as exemplified in DNA repair. *Cell*, **151**, 807–820.
63. Hay,R.T. (2005) SUMO: a history of modification. *Mol. Cell*, **18**, 1–12.
64. Ramachandran,S., Tran,D.D., Klebba-Faerber,S., Kardinal,C., Whetton,A.D. and Tamura,T. (2011) An ataxia-telangiectasia-mutated (ATM) kinase mediated response to DNA damage down-regulates the mRNA-binding potential of THOC5. *RNA*, **17**, 1957–1966.
65. Makhnevych,T., Ptak,C., Lusk,C.P., Aitchison,J.D. and Wozniak,R.W. (2007) The role of karyopherins in the regulated sumoylation of septins. *J. Cell Biol.*, **177**, 39–49.
66. Sydorskyy,Y., Srikumar,T., Jeram,S.M., Wheaton,S., Vizeacoumar,F.J., Makhnevych,T., Chong,Y.T., Gingras,A.C. and Raught,B. (2010) A novel mechanism for SUMO system control: regulated Ulp1 nucleolar sequestration. *Mol. Cell Biol.*, **30**, 4452–4462.
67. Johnson,S.A., Cubberley,G. and Bentley,D.L. (2009) Cotranscriptional recruitment of the mRNA export factor Yra1 by direct interaction with the 3′-end processing factor Pcf11. *Mol. Cell*, **33**, 215–226.
68. MacKellar,A.L. and Greenleaf,A.L. (2011) Cotranscriptional association of mRNA export factor Yra1 with C-terminal domain of RNA polymerase II. *J. Biol. Chem.*, **286**, 36385–36395.
69. Mollapour,M., Fong,D., Balakrishnan,K., Harris,N., Thompson,S., Schuller,C., Kuchler,K. and Piper,P.W. (2004) Screening the yeast deletant mutant collection for hypersensitivity and hyper-resistance to sorbate, a weak organic acid food preservative. *Yeast*, **21**, 927–946.
70. Kawahata,M., Masaki,K., Fujii,T. and Iefuji,H. (2006) Yeast genes involved in response to lactic acid and acetic acid: acidic conditions caused by the organic acids in Saccharomyces cerevisiae cultures induce expression of intracellular metal metabolism genes regulated by Aft1p. *FEMS Yeast Res.*, **6**, 924–936.
71. Mira,N.P., Palma,M., Guerreiro,J.F. and Sa-Correia,I. (2010) Genome-wide identification of Saccharomyces cerevisiae genes required for tolerance to acetic acid. *Microb. Cell Fact.*, **9**, 79.
72. Assenholt,J., Mouaikel,J., Andersen,K.R., Brodersen,D.E., Libri,D. and Jensen,T.H. (2008) Exonucleolysis is required for nuclear mRNA quality control in yeast THO mutants. *RNA*, **14**, 2305–2313.